Journal of Sound and Vibration (2003) **259**(3), 585–603
doi:10.1006/jsvi.2002.5110, available online at http://www.idealibrary.com on IDEAL®

CHAOS, CHAOS CONTROL AND SYNCHRONIZATION OF ELECTRO-MECHANICAL GYROSTAT SYSTEM

Z.-M. Ge and T.-N. Lin

Department of Mechanical Engineering, National Chiao Tung Uuniversity, 1001 *Ta Hsuei road,* 30050 *Hsinchu, Taiwan, Republic of China. E-mail: zmg@cc.nctu.edu.tw*

(*Received* 25 *October* 2001 *and in final form* 8 *April* 2002)

The dynamic behavior of electro-mechanical gyrostat system subjected to external disturbance is studied in this paper. By applying numerical results, phase diagrams, power spectrum, Period-T maps, and Lyapunov exponents are presented to observe periodic and chaotic motions. The effect of the parameters changed in the system can be found in the bifurcation and parametric diagrams. Several methods, the delayed feedback control, adaptive control algorithm (ACA) control are used to control chaos effectively. Anticontrol of chaos destroyed the periodic motions and replaced by chaotic motion effectively by adding constant motor torque and adding periodic motor torque. Finally, synchronization of chaos in the electro-mechanical gyrostat system is studied.

© 2002 Elsevier Science Ltd. All rights reserved.

1. INTRODUCTION

During the past one and a half decades, a large number of studies have shown that chaotic phenomena are observed in many physical systems that possess non-linearity [1, 2]. It was also reported that chaotic motion occurred in many non-linear control systems [3, 4]. Mechatronic integration [5, 7] is interesting research to study in recent years. The advantages of the electro-mechanical system are that it can make the traditional mechanical system easier to be controlled and used. In this paper, continued from reference [8], there are three rotors which are orthogonalized with each other in the gyrostat. The angular momentum of one of the rotors is disturbed by a sinusoidal ripple. Besides, the current of the control-motor in the gyrostat is considered as a state variable. The control-motor can provide a torque which controls the gyrostat to satisfy a purpose we require. The non-linear dynamics, chaotic control and synchronization of this electro-mechanical gyrostat system will be studied in this paper.

A number of modern techniques are used in analyzing the deterministic non-linear system behavior. Computational methods are employed to obtain the characteristics of the non-linear system. By applying numerical results, phase diagrams, power spectrum, period-T maps and Lyapunov exponents are presented to observe periodic and chaotic motions. The effect of the parameters changed in the system can be found in the bifurcation and parametric diagrams. Attention is shifted to the controlling chaos. For this purpose, the delayed feedback control and adaptive control algorithm (ACA) control are used to control chaos. Anticontrol of chaos is used to control the regular motions to chaotic motion. Finally, chaos synchronization [9–11] in the electro -mechanical gyrostat system is studied.

0022-460X/02/$35.00 © 2002 Elsevier Science Ltd. All rights reserved.

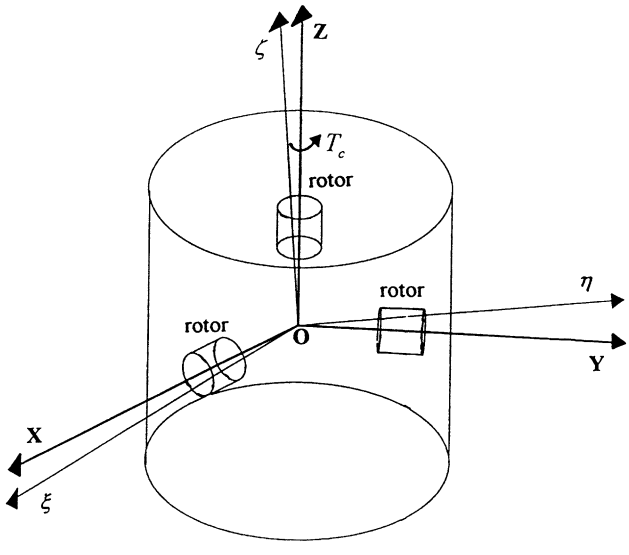

Figure 1. System model.

2. EQUATIONS OF MOTION

The system considered here is depicted in Figure 1. Assume that there are three rotors in a satellite. Let $O\xi\eta\zeta$ be an inertia orthogonal co-ordinate system with origin at mass center O of satellite. Let $OXYZ$ be a rotating orthogonal co-ordinate system with satellite and OX, OY and OZ the three principal axes of inertia respectively. ω_x, ω_y, ω_z are the projection of the angular velocity on the X-, Y-, Z-axis respectively. A, B, C are the principal moments of inertia. The angular moments of rotors h_1, h_2, h_3 are located at OX, OY, OZ. The angular moment of rotor h_3 is presented by a constant and harmonic term $h_3(1 + f\cos\omega t)$, where h_3, f, ω are constants. ω_r is the projection of the angular velocity of the satellite on the X-, Y-, Z-axis which is designed. Add the feedback terms to control the angular velocity $\omega_x\,\omega_y\,\omega_z$ to ω_r. Let $\omega_x = x$, $\omega_y = y$, $\omega_z = z$; then the equation of motion can be expressed as

$$\dot{x} = \frac{(B-C)}{A}yz - \frac{h_3}{A}(1 + f\cos\omega t)y + \frac{h_2}{A}z + \frac{k_1}{A}(\omega_r - x) + \frac{k_2}{A}(\omega_r^3 - x^3),$$

$$\dot{y} = \frac{(C-A)}{B}xz - \frac{h_1}{B}z + \frac{h_3}{B}(1 + f\cos\omega t)x + \frac{k_3}{B}(\omega_r - y) + \frac{k_4}{B}(\omega_r^3 - y^3),$$

$$\dot{z} = \frac{(A-B)}{C}xy + \frac{h_3}{C}f\omega\sin\omega t - \frac{h_2}{C}x + \frac{h_1}{C}y - \frac{b}{C}z + \frac{k_5}{C}(\omega_r - z) + \frac{k_6}{C}(\omega_r^3 - z^3) + \frac{T_c}{C} \qquad (1)$$

equations containing non-linear feedback terms; b is the damping coefficient. $A = 500$, $B = 500, C = 1000$, $h_1 = h_2 = 200$, $h_3 = 250$, $b = 200$, $\omega = 1{\cdot}0$, $k_i\,(i = 1, \ldots, 6) = 1$, $\omega_r = 0$. T_c is the control-motor torque along the output axis of the system to balance the corresponding gyrostat torque. The torque and electric current of the control-motor can be modelled by the following relationship:

$$T_c = K_T I, \quad L\dot{I} + RI = K_a(\omega_r - z) - K_b z, \qquad (2)$$

where $K_T = 300$ denotes the torque constant of the control-motor, $K_a(\omega_r - z)$ is the electromotive force, $K_a = 50$, $K_b z$ is the back electromotive force, $K_b = 1{\cdot}3$, I, R, L, are the current, resistance and inductance of the control-motor, $R = 100$, $L = 2$. Combining

equations (1) and (2), the electro-mechanical gyrostat system equations can be written as

$$\dot{x} = \frac{(B-C)}{A} yz - \frac{h_3}{A}(1 + f\cos\omega t)y + \frac{h_2}{A} z + \frac{k_1}{A}(\omega_r - x) + \frac{k_2}{A}(\omega_r^3 - x^3),$$

$$\dot{y} = \frac{(C-A)}{B} xz - \frac{h_1}{B} z + \frac{h_3}{B}(1 + f\cos\omega t)x + \frac{k_3}{B}(\omega_r - y) + \frac{k_4}{B}(\omega_r^3 - y^3),$$

$$\dot{z} = \frac{(A-B)}{C} xy + \frac{h_3}{C} f\omega \sin\omega t - \frac{h_2}{C} x + \frac{h_1}{C} y - \frac{b}{C} z + \frac{k_5}{C}(\omega_r - z) + \frac{k_6}{C}(\omega_r^3 - z^3) + \frac{K_T}{C} I,$$

$$\dot{I} = \frac{K_a(\omega_r - z)}{L} - \frac{K_b}{L} z - \frac{R}{L} I. \tag{3}$$

3. PHASE PORTRAITS, PERIOD-T MAP AND POWER SPECTRUM

The phase plane is the evolution of a set of trajectories emanating from various initial conditions in the state space. When the solution reaches a stable state, the asymptotic behavior of the phase trajectories is particularly interesting and the transient behavior in the system is neglected. The period-T map, where T is the time period of the forcing, is a better method for displaying the dynamics. Equation (3) is plotted in Figure 2(a)–2(c) for $f = 13{\cdot}6$, $13{\cdot}3$ and $13{\cdot}05$ respectively. Clearly, the motion is periodic. But Figure 2(d), for $f = 12{\cdot}9$, shows the chaotic state. The points of the period-T map become irregular.

Another technique for the identification and characterization of the system is power spectrum. It is often used to distinguish between periodic, quasi-periodic and chaotic behavior for a dynamical system. Any function $x(t)$ may be represented as a superposition of different periodic components. The determination of their relative strength is called spectral analysis. If it is periodic, the spectrum may be a linear combination of oscillations whose frequencies are integer multiples of basic frequency. The linear combination is called a Fourier series. If it is not periodic, the spectrum then must be in terms of oscillations with a continuum of frequencies. Such a representation of the spectrum is called the Fourier integral of $x(t)$. The representation is useful for dynamical analysis. The non-autonomous system is observed by the portraits of the power spectrum in Figure 3(a)–3(c) for periods-1T, $2T$ and $4T$ steady state vibration. S_x is the amplitude of the component in Fourier series expansion for x. As $f = 12{\cdot}9$ chaos occurs, the spectrum is a broad band shown and the peak is still presented at the fundamental frequency shown in Figure 3(d). The noise-like spectrum is the characteristic of a chaotic dynamical system.

4. BIFURCATION DIAGRAM AND PARAMETER DIAGRAM

In the previous section, the information about the dynamics of the non-linear system for specific values of the parameters is provided. The dynamics may be viewed more completely over a range of parameter values. As the parameter is changed, the equilibrium points and periodic motions can be created or destroyed, or their stability can be lost. The phenomenon of sudden change in the motion as a parameter is varied is called bifurcation, and the parameter values at which they occur are called bifurcation points. The bifurcation diagram of the non-linear system of equation is depicted in Figure 4. $f \in [12{\cdot}8, 13{\cdot}7]$ with the incremental value of f is $0{\cdot}001$.

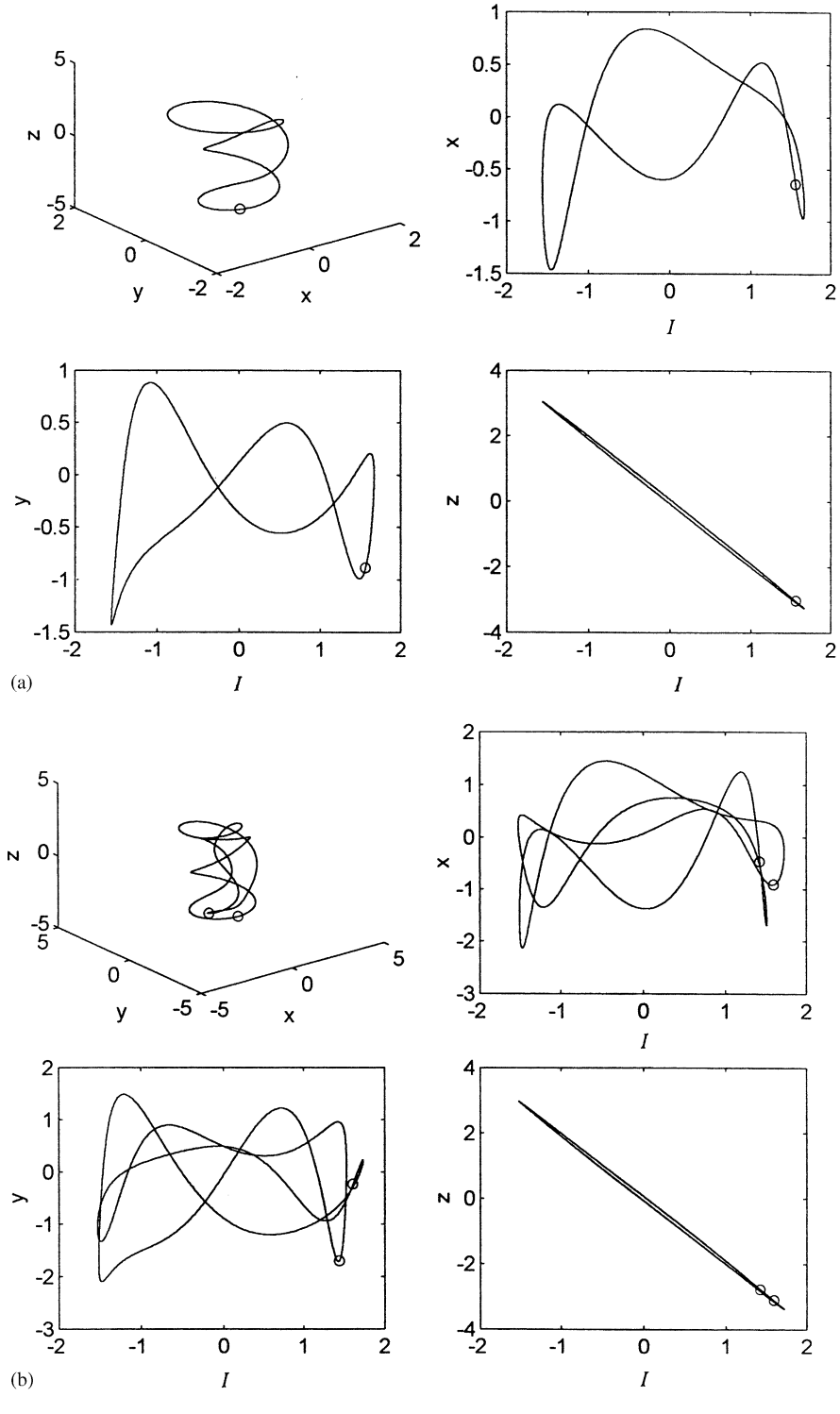

Figure 2. (a) Phase portrait and period-1T map "$\circ$" for $f = 13{\cdot}6$; (b) phase portrait and period-2T map "$\circ$" for $f = 13{\cdot}3$; (c) phase portrait and period-4T map "$\circ$" for $f = 13{\cdot}05$; (d) $f = 12{\cdot}9$, phase portraits and period-T map "$\circ$" of chaos.

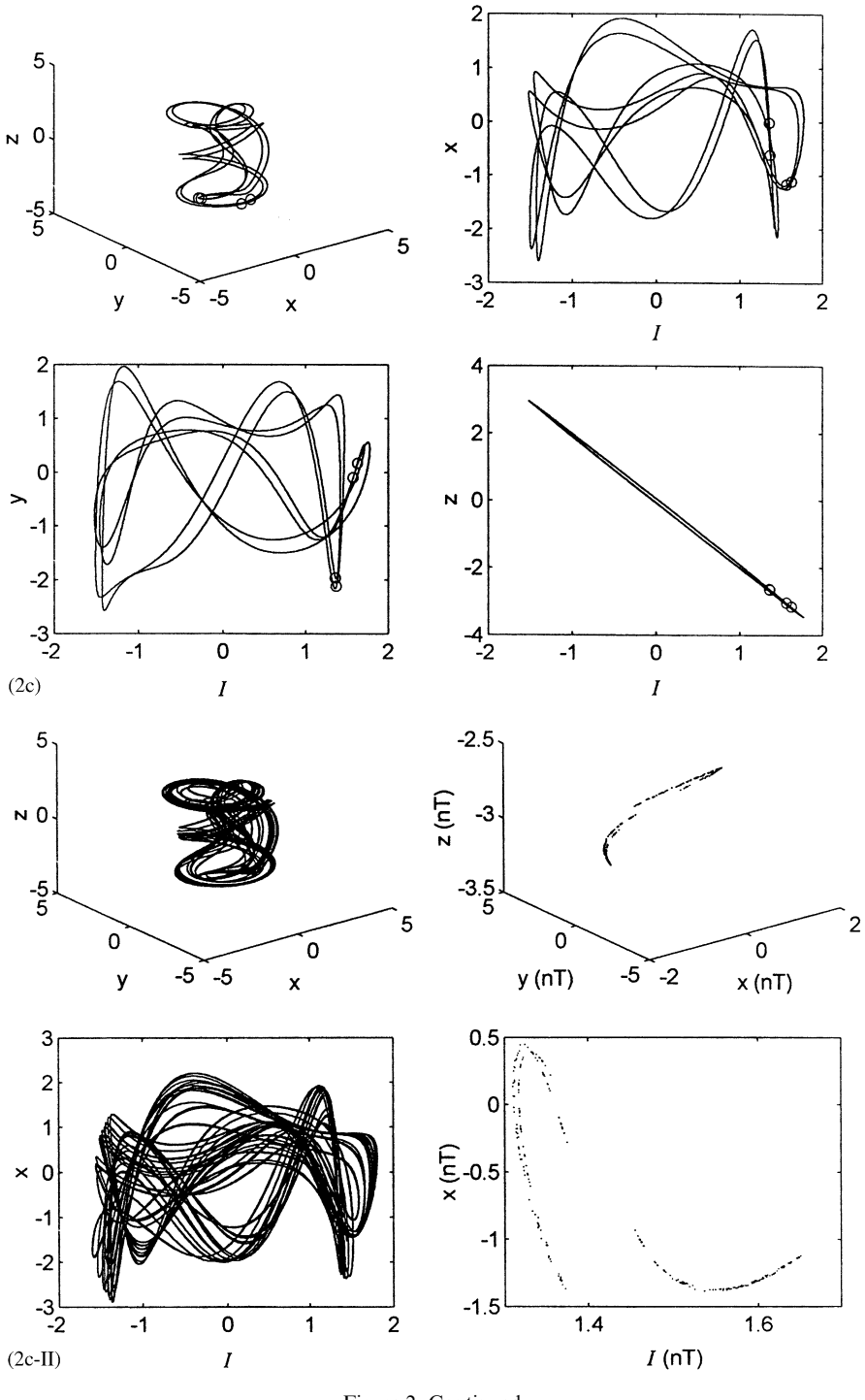

Figure 2. Continued.

Further, the parameter value f versus R and K_T will also be varied to observe the behaviors of bifurcation of the system. Parameter diagrams are shown in Figure 5(a) and 5(b).

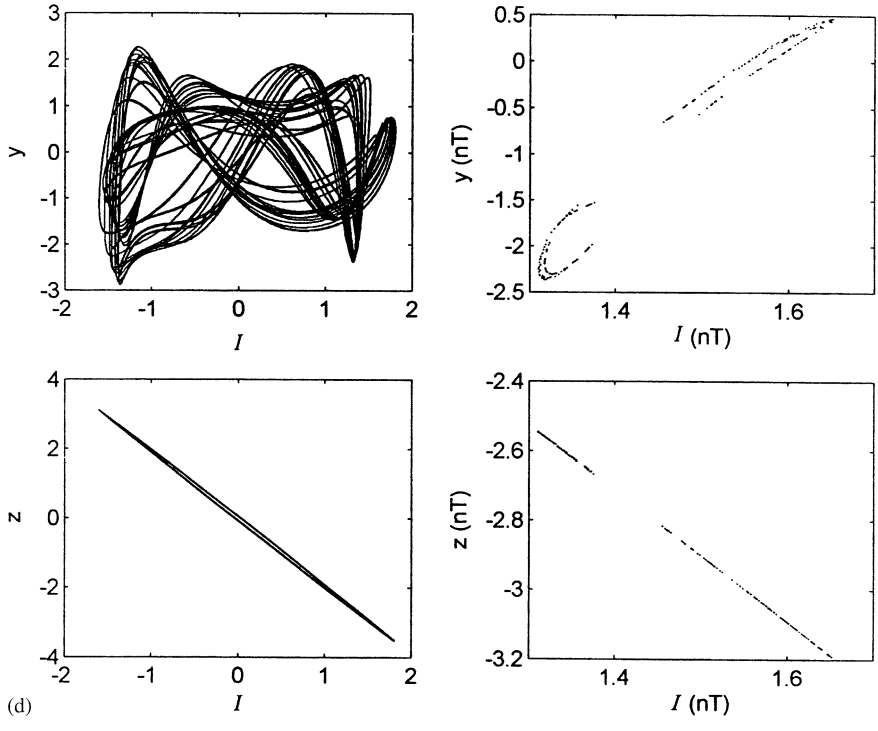

Figure 2. Continued.

5. LYAPUNOV EXPONENT AND LYAPUNOV DIMENSION

The Lyapunov exponent may be used to measure the sensitive dependence upon initial conditions. It is an index for chaotic behavior. Different solutions of a dynamic system, such as fixed points, periodic motions, quasi-periodic motion and chaotic motion can be distinguished by it. If two trajectories start close to one another in phase space, they will move exponentially away from each other for small times on the average. Thus, if d_0 is a measure of the initial distance between the two starting points, the distance is $d(t) = d_0 2^{\lambda t}$. The symbol λ is called Lyapunov exponent. The divergence of chaotic orbits can only be locally exponential, because if the system is bounded, $d(t)$ cannot grow to infinity. A measure of this divergence of orbits is that the exponential grown at many points along a trajectory has to be averaged. When $d(t)$ is too large, a new "nearby" trajectory $d_0(t)$ is defined. The Lyapunov exponent can be expressed as

$$\lambda = \frac{1}{t_N - t_0} \sum_{k=1}^{N} \log_2 \frac{d(t_k)}{d_0(t_{k-1})}. \tag{4}$$

The signs of the Lyapunov exponents provide a qualitative picture of a system dynamics. The criterion is

$$\lambda > 0 \quad \text{(chaotic)}, \qquad \lambda \leqslant 0 \quad \text{(regular motion)}.$$

The periodic and chaotic motions can be distinguished by the bifurcation diagram, while the quasi-periodic motion and chaotic motion may be confused. However, they can be distinguished by the Lyapunov exponent method. The maximum Lyapunov exponent of the non-linear dynamic system is plotted in Figure 6 as $f = 12{\cdot}8 - 13{\cdot}7$.

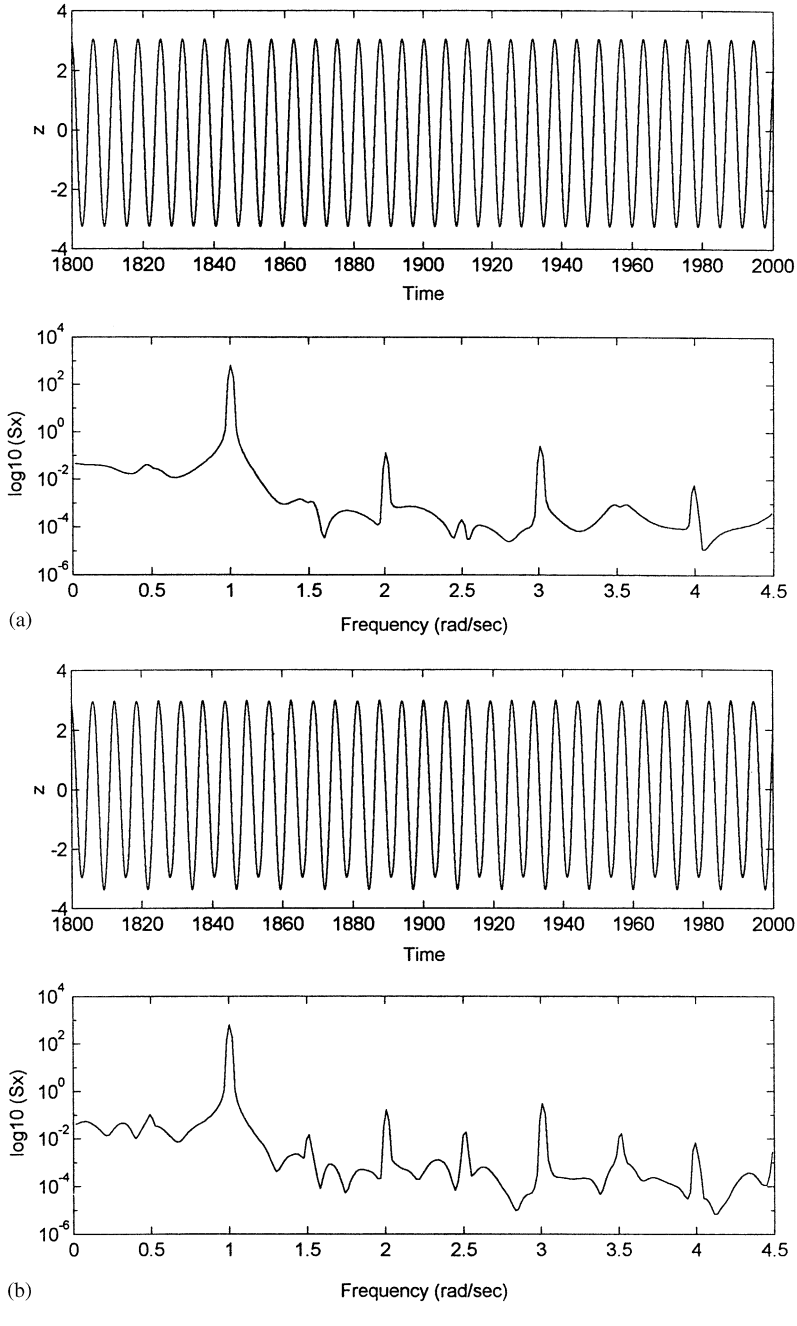

Figure 3. (a) Power spectrum and time history of period-1T for $f = 13{\cdot}6$; (b) power spectrum and time history of period-2T for $f = 13{\cdot}3$; (c) power spectrum and time history of period-4T for $f = 13{\cdot}05$; (d) power spectrum and time history of chaos for $f = 12{\cdot}9$.

There are a number of different fractional-dimension-like indices, e.g. the information dimension, Lyapunov dimension and correlation exponent, etc.; the difference between them is often small. The Lyapunov dimension is a measure of the complexity of the

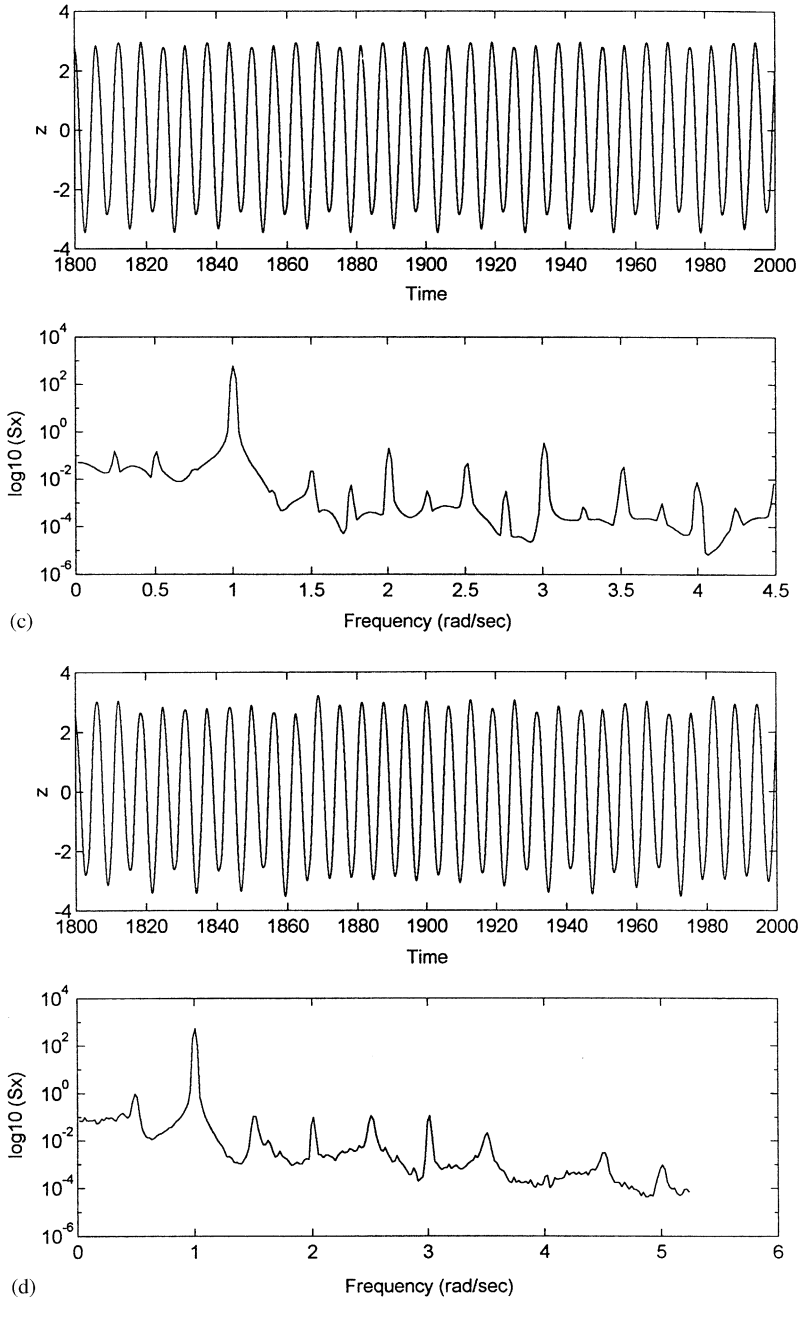

Figure 3. Continued.

attractor. It has been developed [12] that the Lyapunov dimension d_L is introduced as

$$d_L = j + \frac{\sum_{i=1}^{j} \lambda_i}{|\lambda_{j+1}|}, \tag{5}$$

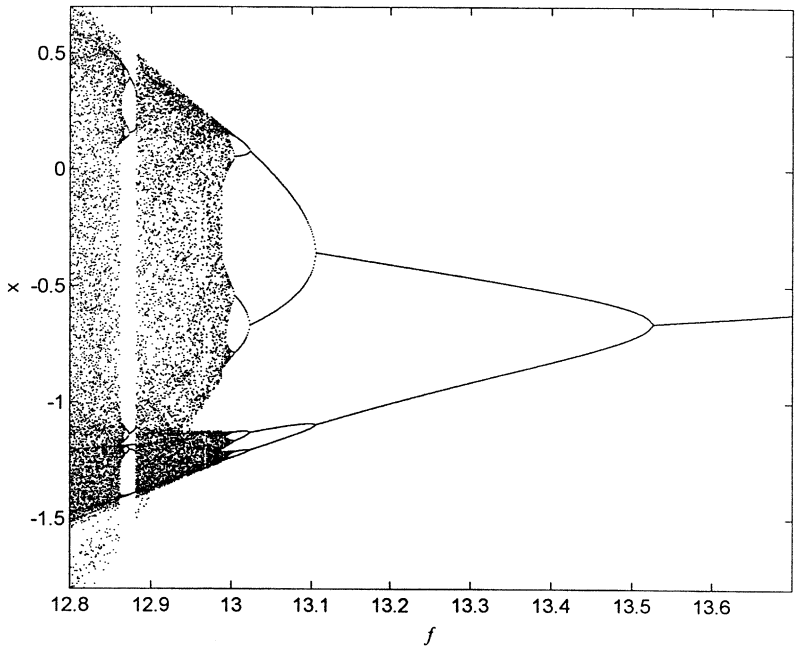

Figure 4. Bifurcation diagram of f versus x.

where j is defined by the condition

$$\sum_{i=1}^{j} \lambda_i > 0 \quad \text{and} \quad \sum_{i=1}^{j+1} \lambda_i < 0.$$

The Lyapunov dimension for a strange attractor is a non-integer number. The Lyapunov dimension and the Lyapunov exponent of the non-linear system are listed in Table 1 for different values of f.

6. CONTROLLING CHAOS

Several kinds of interesting non-linear dynamic behavior of the system are studied in previous sections. They have shown that the forced system exhibited both regular and chaotic motion. Usually chaos is unwanted or undesirable.

In order to improve the performance of a dynamic system or avoid the chaotic phenomena, we need to control a chaotic system to a periodic motion which is beneficial for working with a particular condition. It is thus of great practical importance to develop suitable control methods. Very recently much interest has been focused on this type of problem—controlling chaos [13–19]. For this purpose, the delayed feedback control and ACAs are used to control chaos. Anticontrol of chaos [14, 20] is interesting, non-traditional, and very challenging. In this section, two simple explicit formulations have been used to study anticontol of chaos. As a result, the chaotic system can be controlled.

6.1. CONTROLLING OF CHAOS BY DELAYED FEEDBACK CONTROL

Let us consider a dynamic system which can be simulated by ordinary differential equations. We imagine that the equations are unknown, but some scalar variable can be measured as a system output. The idea of this method is that the difference $D(t)$ between

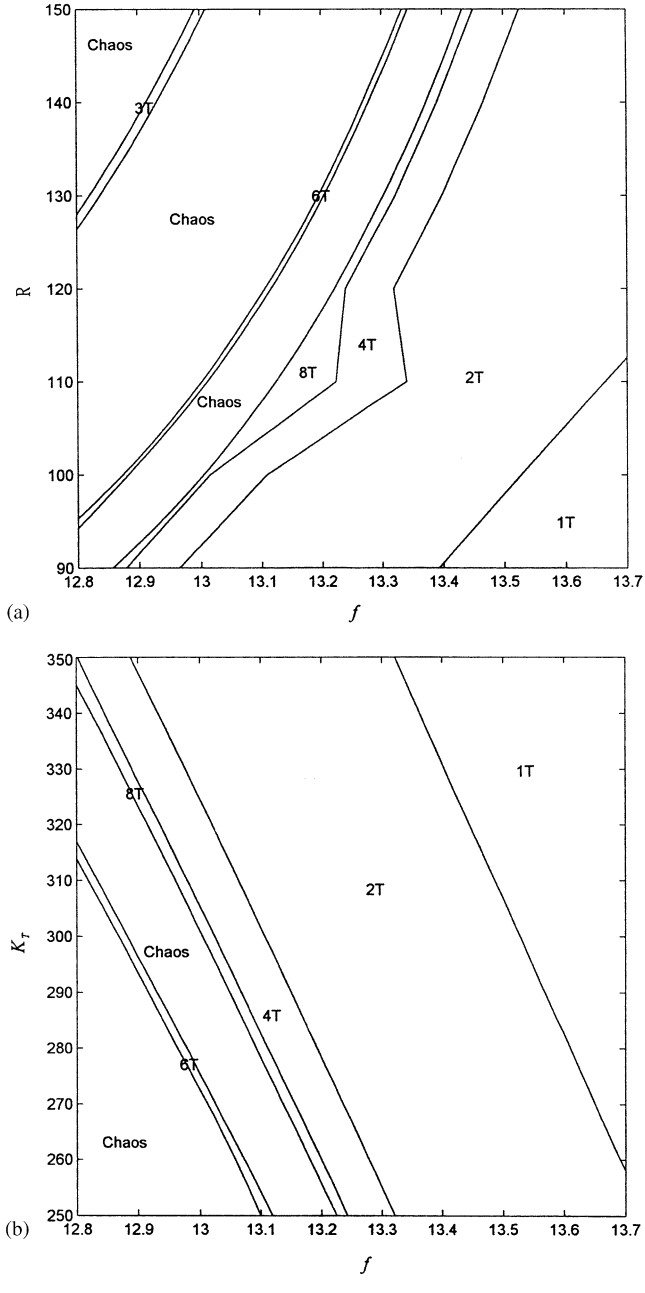

Figure 5. Parameter diagram of (a) f versus R and (b) f versus K_T.

the delayed output signal $z(t-\tau)$and the output signal $z(t)$ is used as a control signal. In other words, we used a perturbation of the form

$$F(t) = K_A[z(t-\tau) - z(t)] = KD(t), \tag{6}$$

where τ is delay time. Choose an appropriate weight K_A and τ of the feedback and one can achieve the periodic state. If $K_A = 20{\cdot}5$, 13, 9 and $\tau = 2\pi/\omega$, the results are shown in Figure 7(a)–7(c).

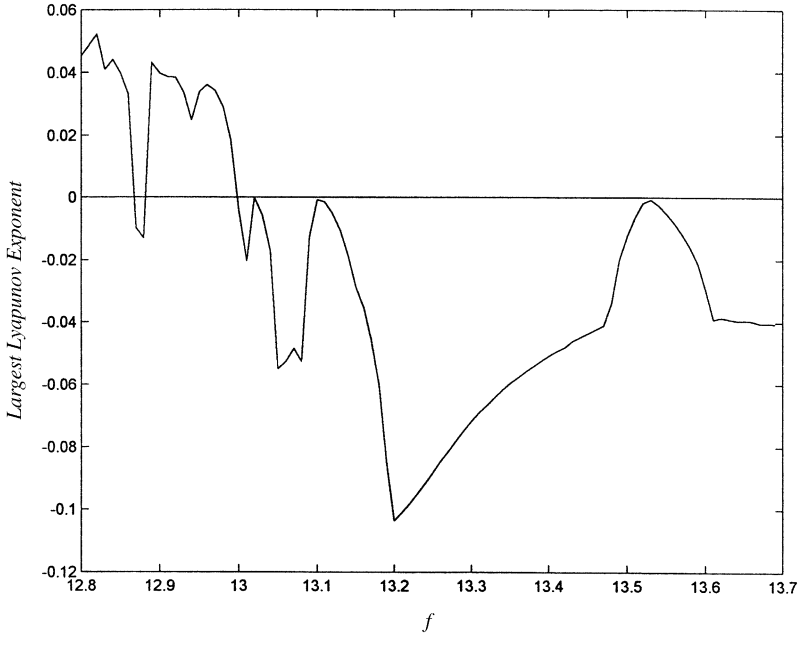

Figure 6. Largest Lyapunov exponents for f between 12·8 and 13·7.

TABLE 1

Lyapunov exponents and Lyapunov dimensions of the system for different f

f	λ_1	λ_2	λ_3	λ_4	d_L	
13.6	−0.0312	−0.0515	−0.2981	−8.8978	1	Period-1
13.3	−0.0746	−0.0809	−0.2290	−8.8978	1	Period-2
13.05	−0.0620	−0.0654	−0.2615	−8.8977	1	Period-4
12.9	0.0383	−0.1517	−0.2764	−8.8977	1.252	Chaos

This control is achieved by the use of the output signal, which is fed back into the system. The difference between the delayed output signal and the output signal itself is used as a control signal. Only a simple delay line is required for this feedback control. To achieve the periodic motion of the system, two parameters, namely, the time of delay τ and the weight K_A of the feedback, should be adjusted. In this paper, the parameter τ is the value that causes the controlling gain K_A a minimum value for controlling the system to periodic motion. As a result, minimum energy is costed when other conditions are the same.

6.2. CONTROLLING CHAOS BY ACA

Huberman and Lumer [17] have suggested a simple and effective ACA which utilizes an error signal proportional to the difference between the goal output and actual output of the system. The error signal governs the change of parameters of the system, which

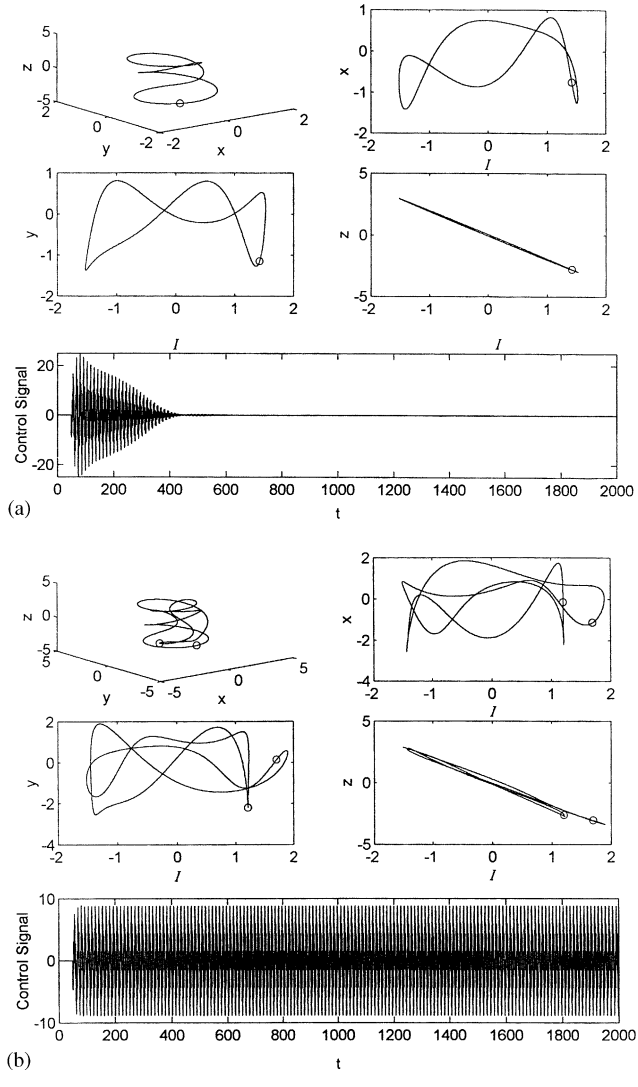

Figure 7. (a) $K_A = 20{\cdot}5$, the period-1T motion of the system after delay feedback control; (b) $K_A = 13$, the period-2T motion of the system after delay feedback control; (c) $K_A = 9$, the period-4T motion of system after delay feedback control.

readjusts so as to reduce the error to zero. This method can be explained briefly: the system motion is set back to a desired state X_s by adding dynamics to the control parameter P through the evolution equation

$$\dot{\boldsymbol{P}} = K_B G(X - X_s), \tag{7}$$

where the function G is proportional to the difference between X_s and the actual output X, and K_B indicates the stiffness of the control. The function G could be either linear or nonlinear. In order to convert the dynamics of system (3) from chaotic motion to the desired periodic motion X_s, the chosen parameter f is perturbed as

$$\dot{f} = K_B(X - X_s). \tag{8}$$

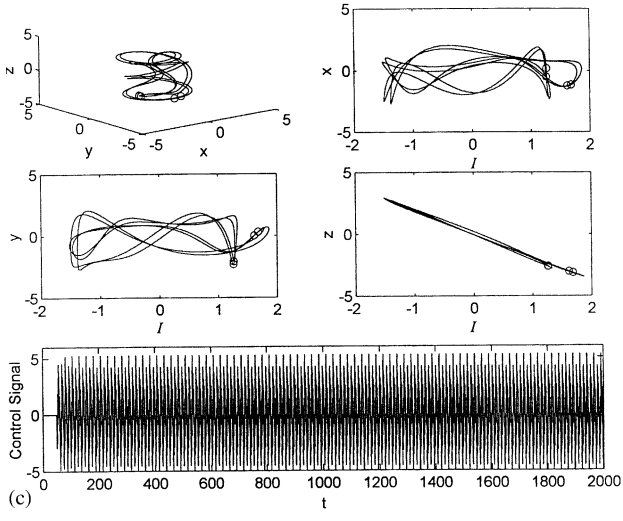

Figure 7. Continued

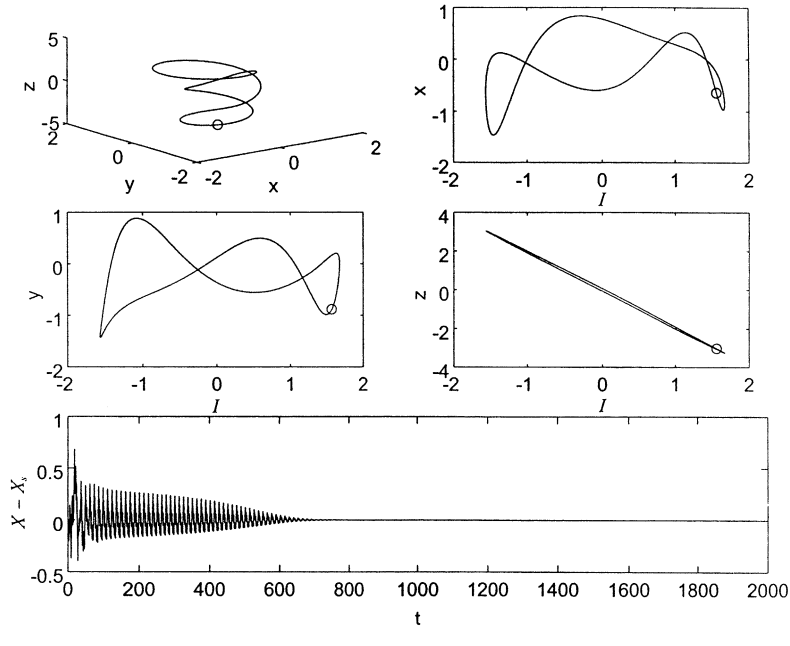

Figure 8. Period-1T motion of the system after adaptive control.

If $K_B = 0{\cdot}2$, the system can reach the period-1T motion and is shown in Figure 8. The parameter K_B is the minimum effective value to control the chaotic motion to periodic motion. For smaller parameters the adaptive control becomes ineffective.

In this paper, the delayed feedback control is more effective than the adaptive control. By using the delayed feedback control, the chaotic motion of the original system can be controlled to period-1T, Period-2T and Period-4T motions. But, by using the adaptive

control, the chaotic motion of the original system only can be controlled to period-4T motion. For the controlling purpose, the delayed feedback control algorithm gives better results than the adaptive control.

6.3. ANTICONTROL OF CHAOS

Anticontrol of chaos is whether or not one can make an arbitrarily given system chaotic or enhance the existing chaos of a chaotic system by using arbitrarily small controls. This implies that the regular behaviors will be destroyed and replaced by chaotic behavior. In the real world, chaotic behavior is important. Examples include liquid mixing, human heartbeat regulations, resonance prevention in mechanical systems and secure communications. In this subsection, adding constant motor torque and adding period motor torque methods are used to anticontrol of chaos.

6.3.1. *Adding constant motor torque to anticontrol of chaos*

Interestingly, one can even add just a constant term to control the regular attractor to a chaotic one in a typical non-linear non-autonomous system. It ensures effective anticontrol of chaos in a very simple way.

Consider the effect of the constant motor torque M added to the right-hand side of the third equation of equation (3). If $M = 0{\cdot}95$, the bifurcation diagram of the system is shown in Figure 9(a) and the largest Lyapunov exponent is shown in Figure 9(c).

6.3.2. *Adding periodic motor torque to anticontrol of chaos*

For our purpose, the periodic motor torque, $N\sin(\varpi t + \phi)$, is added to the right-hand side of the third equation of equation (3), the system can then be investigated by numerical solution. One case to examine is the change in the dynamics of the system as $N = 10$, $\varpi = 1{\cdot}5$, $\phi = 0$. Figure 9(b) and 9(d) presents the bifurcation diagram and the largest Lyapunov exponent diagram of the system after anticontrol of chaos. Obviously, in both methods, the regular behaviors (periods-1T, 2T, 4T) in Figure 4 disappeared and were replaced by chaotic behavior.

The chaotic motion of this gyrostat system has practical significance. For instance, the gyrostat system can be seen as a missile. When the defense missile is tracking the attack missile, if the attack missile is in the chaotic motion as a result of the integration of angular velocity components in our system, it can be hardly reached by the defense missile. Since chaotic motion is expected in this case, the anticontrols of chaos of the gyrostat system are also useful.

7. SYNCHRONIZATION OF CHAOS

The concept of chaos synchronization emerged much later—not until the gradual realization of the usefulness of chaos by scientists and engineers. Chaotic signals are usually broad band and noise-like. Because of this property, synchronized chaotic systems can be used as cipher generators for secure communication. Several methods of synchronization have been studied in many theoretical model equations and electrical systems [9–11, 21], recently. In this section, chaos synchronization for the electromechanical gyrostat system will be studied.

In previous researches, the studies are well known, such as Lorenz system [22, 23], Rössler system [22, 24] and Chua's circuits system [25, 26], etc. with linear coupling term. Following these researches, in this paper, the chaos synchronization of the gyrostat system

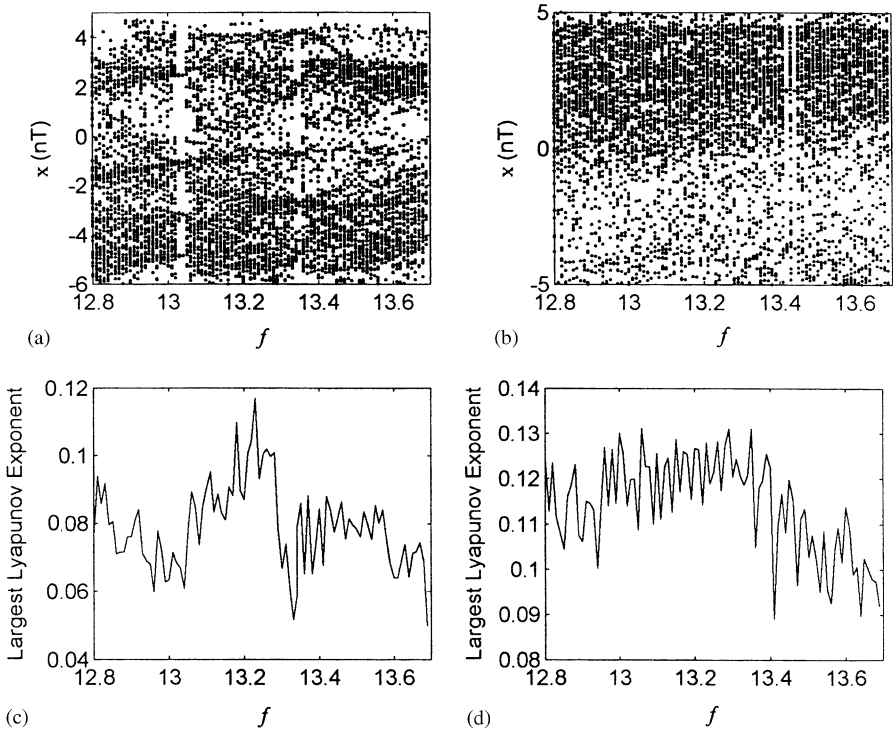

Figure 9. Bifurcation diagram after anticontrol of chaos by adding: (a) constant motor torque; (b) periodic motor torque (the largest Lyapunov exponent diagram after anticontrol of chaos), (c) constant motor torque; and (d) periodic motor torque.

is studied with the linear coupling term also. Two new kinds of coupling terms (equation (13): sinusoid feedback term, and equation (14): exponential feedback term) were created because of their simplicity and clarity.

Equation (3) can be expressed as two identical subsystems

$$\text{drive:} \quad \begin{cases} \dot{x}_1 = f_1(x_1, y_1, z_1), \\ \dot{y}_1 = f_2(x_1, y_1, z_1), \\ \dot{z}_1 = f_3(x_1, y_1, z_1, I_1), \\ \dot{I}_1 = f_4(z_1, I_1), \end{cases} \tag{9}$$

$$\text{response:} \quad \begin{cases} \dot{x}_2 = f_1(x_2, y_2, z_2), \\ \dot{y}_2 = f_2(x_2, y_2, z_2), \\ \dot{z}_2 = f_3(x_2, y_2, z_2, I_2), \\ \dot{I}_2 = f_4(z_2, I_2). \end{cases} \tag{10}$$

The chaotic attractor can be obtained for the initial conditions $(x_1(0), y_1(0), z_1(0), I_1(0)) = (0{\cdot}1,\ 0{\cdot}2,\ 0{\cdot}3,\ 0{\cdot}0)$ and $(x_2(0), y_2(0), z_2(0), I_2(0)) = (1,\ 2,\ 3,\ 0{\cdot}1)$.

The coupling terms are added in the response system as

$$\text{response:} \quad \begin{cases} \dot{x}_2 = f_1(x_2, y_2, z_2), \\ \dot{y}_2 = f_2(x_2, y_2, z_2), \\ \dot{z}_2 = f_3(x_2, y_2, z_2, I_2) + F(z_1, z_2), \\ \dot{I}_2 = f_4(z_2, I_2). \end{cases} \tag{11}$$

$F(z_1, z_2)$ have several forms:

(A) *linear feedback term*

$$F(z_1, z_2) = \varepsilon(z_1 - z_2), \tag{12}$$

(B) *sinusoid feedback term*

$$F(z_1, z_2) = \varepsilon \sin(z_1 - z_2), \tag{13}$$

(C) *exponential feedback term*

$$F(z_1, z_2) = \varepsilon[\exp(z_1 - z_2) - 1]. \tag{14}$$

The coupling strength ε of all methods is 0·7 and the results of synchronization are shown in Figures 10–12.

(D) *adaptive feedback synchronization*

In Section 6.2, adaptive control schemes can direct a chaotic trajectory to stable orbits, but not unstable orbits. Therefore, it is possible to combine the feedback method for chaos synchronization [14].

In response (11), $F(z_1, z_2) = \varepsilon(z_1 - z_2)$ and take the adaptive control scheme:

$$\dot{K}_T = k_D(I_1 - I_2), \tag{15}$$

where K_T is the system parameter and k_D is a constant adaptive control gain to design. Figure 13 shows the results of chaos synchronization after using this method when $\varepsilon = 0{\cdot}7$, $k_D = 1$.

To study the efficacy of the synchronization strategy, was numerically computed the value of f for which stable synchronization is achieved. For this purpose, synchronization time (ST) [11] is considered. The error signal $E(t)$ is given by

$$\begin{aligned} E(t) = {} & |x_1 - x_2| + |y_1 - y_2| + |z_1 - z_2| + |I_1 - I_2| + |\dot{x}_1 - \dot{x}_2| \\ & + |\dot{y}_1 - \dot{y}_2| + |\dot{z}_1 - \dot{z}_2| + |\dot{I}_1 - \dot{I}_2|. \end{aligned} \tag{16}$$

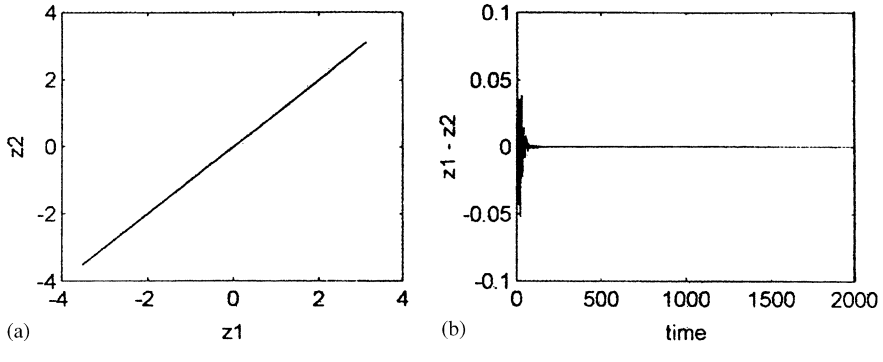

Figure 10. Synchronization of chaos by the linear feedback method $F(z_1, z_2) = \varepsilon(z_1 - z_2)$: (a) relation between z_1 and z_2, (b) error between z_1 and z_2.

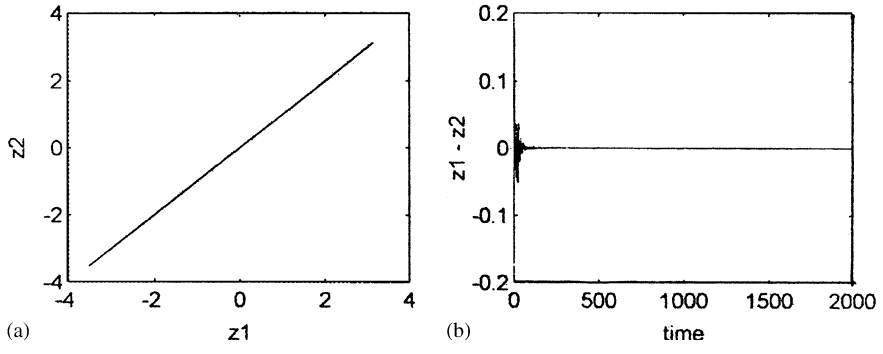

Figure 11. Synchronization of chaos by the sinusoid feedback method $F(z_1, z_2) = \varepsilon \sin(z_1 - z_2)$: (a) relation between z_1 and z_2; (b) error between z_1 and z_2.

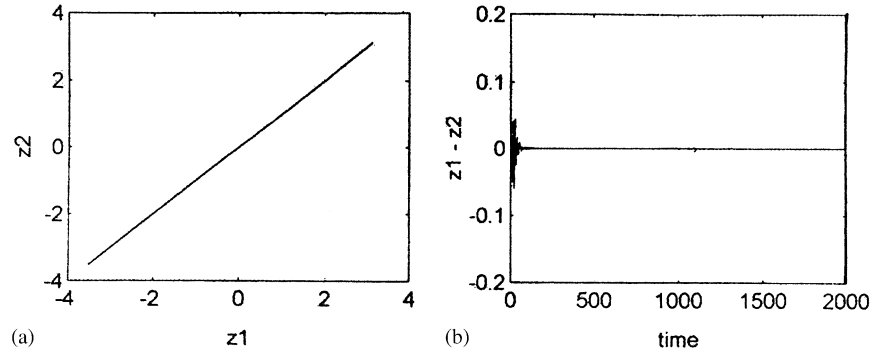

Figure 12. Synchronization of chaos by the exponential feedback method $F(z_1, z_2) = \varepsilon[\exp(z_1 - z_2) - 1]$: (a) relation between z_1 and z_2; (b) error between z_1 and z_2.

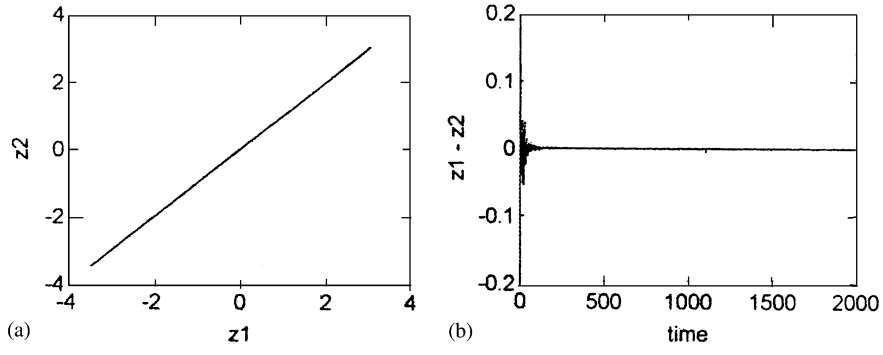

Figure 13. Synchronization of chaos by the adaptive feedback method: (a) relation between z_1 and z_2; (b) error between z_1 and z_2.

ST of the system by using the above methods is shown in Figure 14. In the above four methods, the ST of the adaptive feedback method is smaller than other methods, obviously.

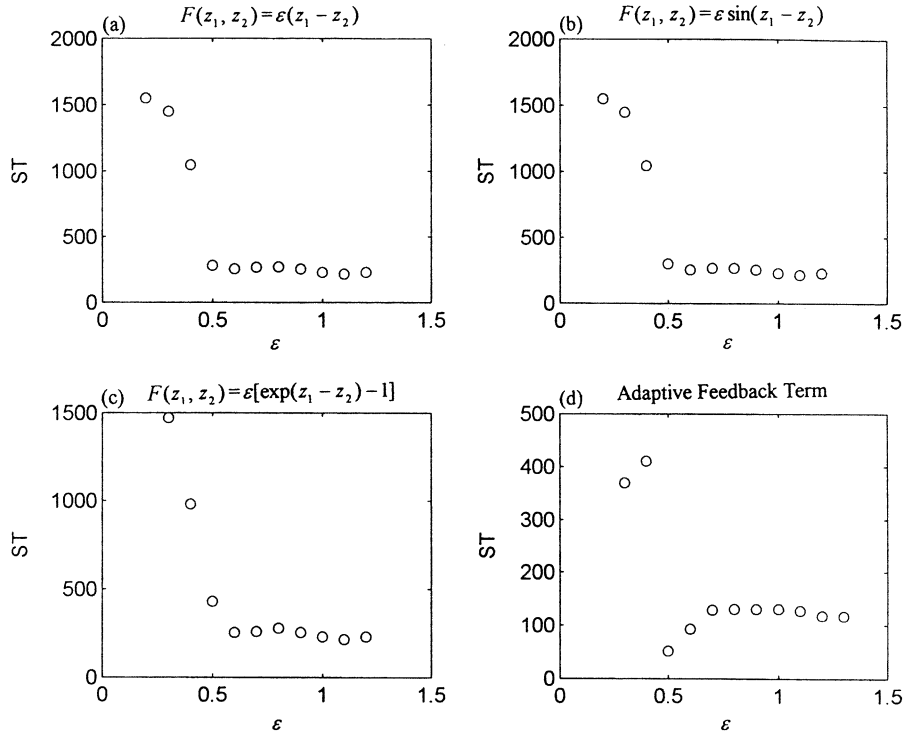

Figure 14. Synchronization time (ST) versus ε for (a) linear feedback term, (b) sinusoid feedback term, (c) exponential feedback term, and (d) adaptive feedback methods.

8. CONCLUSIONS

The dynamic system of the electro-mechanical gyrostat system exhibits a rich variety of non-linear behavior as certain parameters vary. Due to the effect of non-linearity, regular or chaotic motions may occur. In this paper, computational methods have been employed to study the dynamical behavior of the non-linear system.

The periodic and chaotic motions of the nonautonomous system are obtained by numerical methods such as power spectrum, period-T map and Lyapunov exponents. Many non-linear and chaotic phenomena have been displayed in bifurcation diagrams. More information on the behavior of the periodic and the chaotic motion can be found in parametric diagrams. The changes of parameter play a major role for the non-linear system. Chaotic motion is the motion which has a sensitive dependence on the initial condition in deterministic physical systems. The chaotic motion has been detected by using Lyapunov exponents and Lyapunov dimensions. Although the results of the computer simulation have some errors, the conclusions match the bifurcation diagrams.

The presence of chaotic behavior is generic for certain non-linearities, ranges of parameters and external force. Also quenching of the chaos is presented, so as to improve the performance of a dynamical system. The delayed feedback control, adaptive control algorithm and anticontrol of chaos are presented.

Synchronization of chaos has been presented by adding linear feedback term, adding sinusoid feedback term, adding exponential feedback term and adaptive feedback methods.

ACKNOWLEDGMENTS

This research was supported by the National Science Council, Republic of China, under Grant Number NSC 89-2212-E-009-068.

REFERENCES

1. F. C. Moon 1992 *Chaotic and Fractal Dynamics*. New York: Wiley.
2. H. K. Khalil 1996 *Non-linear System*. Englewood Cliffs, NJ: Prentice-Hall.
3. R. W. Brockett 1982 *Proceedings of the IEEE 2lst Conference on Decision and Control*, 932–936. On conditions leading to chaos in feedback systems.
4. P. Holmes 1983 *Proceedings of the IEEE 22nd Conference Decision and Control*, 365–370. Bifurcation and chaos in a simple feedback control system.
5. W. Bolton 1999 *Mechatronics*, New York: Addison Wesley Longman Limited.
6. Fraser, Charles and Miline John 1994 *Elecro-Mechanical Engineering*. UK: McGraw-Hill International.
7. Dobrivojie Popovic and Ljubo Vlacic 1999 *Mechatronics in Engineering Design and Product Development*. New York: Marcel Dekker.
8. Z.-M. Ge and T.-N. Lin 2002 *Journal of Sound and Vibration* **251**, 519–542. Chaos, chaos control and synchronization of gyrostat system.
9. M. P. Louis and L. C. Thomas 1990 *Physical Review Letters* **64**, 821–824. Synchronization in chaotic systems.
10. F. Ricardo, S. P. Gualberto 1999 *Physics Letter A* **262**, 50–60. On the chaos synchronization phenomena.
11. S. Paul Raj, S. Rajasekar, K. Murali 1999 *Physics Letters A* **264**, 283–288. Coexisting chaotic attractors, their basin of attractions and synchronization of chaos in two coulped duffing oscillators.
12. P. Frederickson, J. L. Kaplan, E. D. Yorke and J. A. Yorke 1983 *Journal of Differential Equations* **49**, 185–207. The Liapunov dimension of strange attractors.
13. S. Sinha, R. Ramaswamy and J. S. Rao, 1991 *Physica D* **43**, 118–128. Adaptive control in non-linear dynamics.
14. G. Chen and X. Dong 1998 *From Chaos to Order*. Singapore: World Scientific.
15. Y. Braiman and I. Goldhirsh, 1991 *Phys. Rev. Lett.* **66**, 2545–2548. Taming chaotic dynamics with weak periodic perturbations.
16. E. Ott, C. Grebogi and J. A. Yorke 1990 *Phys. Rev. Lett.* **64**, 1196–1199. Controlling chaos.
17. B. A. Huberman and Lumer 1990 *IEEE Transaction on Circuits and Systems* **37**, 547–550. Dynamics of adaptive system.
18. M. Lakshmanan and K. Murali 1996 *Chaos in Non-linear Oscillators: Controlling and Synchronization*. Singapore: World Scientific.
19. T. Kapitaniak *Controlling Chaos*. 1996 London: Academic Press.
20. Xiao Fan Wang, Guanrong Chen and Xinghuo Yu 2000 *Chaos* **10**, 771–779. Anticontrol of chaos in continuous-time systems via time-delay feedback.
21. Hua-Wei Yin, Jian-Hua Dai and Hong-Jun Zhang 1998 *Physical Review E* **58**, 5683–5688. Phase effect of two coupled periodically driven Duffing oscillators.
22. L. M. Pecora and T. L. Carroll 1990 *Phys. Rev. Lett.* **64**, 821–823. Synchronization in chaotic systems.
23. J. K. John and R. E. Amritkar 1994 *Int'l J. of Bifur. Chaos* **4**, 1687–1695. Synchronization by feedback and adaptive control.
24. L. Kocarev, U. Parlitz, T. Stojanovski and L. Panovski 1996 *Proceedings of the IEEE International Symposium on Circuits and Systems, Atlanta, GA*, Vol. 3, 116–119. Generalized synchronization of chaos.
25. C. W. Wu, T. Yang and L. O. Chua 1996 *International Journal of Bifurcation and Chaos* **6**, 455–471. On adaptive synchronization and control of non-linear dynamical systems.
26. A. K. Kozlov, V. D. Shalfeev and L. O. Chua 1996 *International Journal of Bifurcation and Chaos* **6**, 569–580. Exact synchronization of mismatched chaotic systems.